

## Accepted Manuscript

Discovery, design, and synthesis of indole-based EZH2 inhibitors

Victor S. Gehling, Rishi G. Vaswani, Christopher G. Nasveschuk, Martin Duplessis, Priyadarshini Iyer, Srividya Balasubramanian, Feng Zhao, Andrew C. Good, Robert Campbell, Christina Lee, Les A. Dakin, Andrew S. Cook, Alexandre Gagnon, Jean-Christophe Harmange, James E. Audia, Richard T. Cummings, Emmanuel Normant, Patrick Trojer, Brian K. Albrecht

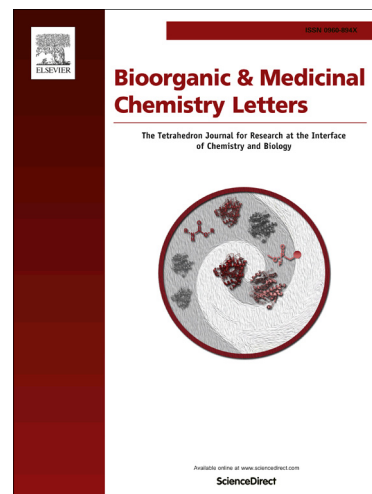
PII: S0960-894X(15)00649-6  
DOI: <http://dx.doi.org/10.1016/j.bmcl.2015.06.056>  
Reference: BMCL 22846

To appear in: *Bioorganic & Medicinal Chemistry Letters*

Received Date: 4 May 2015  
Revised Date: 11 June 2015  
Accepted Date: 15 June 2015

Please cite this article as: Gehling, V.S., Vaswani, R.G., Nasveschuk, C.G., Duplessis, M., Iyer, P., Balasubramanian, S., Zhao, F., Good, A.C., Campbell, R., Lee, C., Dakin, L.A., Cook, A.S., Gagnon, A., Harmange, J-C., Audia, J.E., Cummings, R.T., Normant, E., Trojer, P., Albrecht, B.K., Discovery, design, and synthesis of indole-based EZH2 inhibitors, *Bioorganic & Medicinal Chemistry Letters* (2015), doi: <http://dx.doi.org/10.1016/j.bmcl.2015.06.056>

This is a PDF file of an unedited manuscript that has been accepted for publication. As a service to our customers we are providing this early version of the manuscript. The manuscript will undergo copyediting, typesetting, and review of the resulting proof before it is published in its final form. Please note that during the production process errors may be discovered which could affect the content, and all legal disclaimers that apply to the journal pertain.



**Graphical Abstract**

To create your abstract, type over the instructions in the template box below.  
Fonts or abstract dimensions should not be changed or altered.

**Discovery, design, and synthesis of indole-based EZH2 inhibitors.**

Leave this area blank for abstract info.

Victor S. Gehling, Rishi G. Vaswani, Christopher G. Nasveschuk, Martin Duplessis, Priyadarshini Iyer, Srividya Balasubramanian, Feng Zhao, Andrew C. Good, Robert Campbell, Christina Lee, Les A. Dakin, Andrew S. Cook, Alexandre Gagnon, Jean-Christophe Harmange, James E. Audia, Richard T. Cummings, Emmanuel Normant, Patrick Trojer, Brian K. Albrecht.





## Discovery, design, and synthesis of indole-based EZH2 inhibitors.

Victor S. Gehling<sup>\*</sup>, Rishi G. Vaswani, Christopher G. Nasveschuk, Martin Duplessis, Priyadarshini Iyer, Srividya Balasubramanian, Feng Zhao, Andrew C. Good, Robert Campbell, Christina Lee, Les A. Dakin, Andrew S. Cook, Alexandre Gagnon, Jean-Christophe Harmange, James E. Audia, Richard T. Cummings, Emmanuel Normant, Patrick Trojer and Brian K. Albrecht.

Constellation Pharmaceuticals, Inc., 215 First Street, Cambridge, MA, 02142, USA.

### ARTICLE INFO

### ABSTRACT

#### Article history:

Received

Revised

Accepted

Available online

#### Keywords:

EZH2

PRC2

Histone methyltransferase

Epigenetics

Pyridone

The discovery and optimization of a series of small molecule EZH2 inhibitors is described. Starting from dimethylpyridone HTS hit (**2**), a series of indole-based EZH2 inhibitors were identified. Biochemical potency and microsomal stability were optimized during these studies and afforded compound **22**. This compound demonstrates nanomolar levels of biochemical potency ( $IC_{50} = 0.002 \mu M$ ), cellular potency ( $EC_{50} = 0.080 \mu M$ ), and afforded tumor regression when dosed (200 mpk SC BID) in an EZH2 dependent tumor xenograft model.

2009 Elsevier Ltd. All rights reserved.

<sup>\*</sup> Corresponding author. Tel.: +1-617-714-0540; fax: +1-617-577-0472; e-mail: [victor.gehling@constellationpharma.com](mailto:victor.gehling@constellationpharma.com)

Post-translational modifications of histones are important for the dynamic regulation of chromatin structure and transcription of genetic material.<sup>1</sup> Improper regulation of histone “marks” play an important role in the initiation and progression of certain diseases, in particular cancer. In this context, the histone lysine methyltransferase Enhancer of Zeste Homolog 2 (EZH2), the catalytic subunit of the Polycomb Repressive Complex 2 (PRC2), is involved in transcriptional silencing of targeted genes by catalyzing the methylation of the  $\epsilon$ -NH<sub>2</sub> motif of histone H3 lysine 27 (H3K27).<sup>2</sup> Studies have shown that EZH2 is significantly overexpressed in a wide range of human cancers whereby the relative EZH2 expression level correlates well with cancer stage and poor prognosis.<sup>3,4</sup> Additionally, recurrent mono-allelic gain of function mutations of residues, such as Y641, A677 and A687, within the EZH2 catalytic domain have been observed in germinal center B-cell like diffuse large B-cell lymphoma (GCB-DLBCL) and follicular lymphoma.<sup>5-9</sup> It follows that the inhibition of EZH2 activity holds promise as a potential treatment for cancer.<sup>10</sup>

In this context we and others embarked on the discovery and optimization of inhibitors of the catalytic activity of EZH2. Through these efforts a variety of small molecule inhibitors of EZH2 have been described which produce robust phenotypes both *in vitro* and *in vivo* (Figure 1).<sup>11-19</sup>

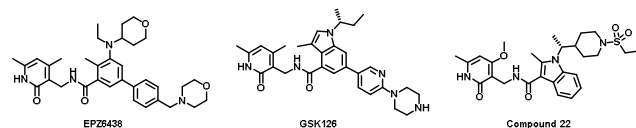


Figure 1. Reported EZH2 inhibitors.

We previously reported **1** as an effective tool compound that produced a characteristic EZH2 inhibitory phenotype in KARPAS-422 lymphoma cells.<sup>20</sup> Unfortunately, the pharmacokinetic (PK) profile for **1** was not suitable for further evaluation of EZH2 inhibition in rodent disease models. Herein we describe our efforts towards the successful identification of a small molecule suitable for the evaluation of EZH2 inhibition *in vivo*.

As part of our ongoing program to discover and develop clinically relevant EZH2 inhibitors, we assessed other chemotypes identified through diversity screening such as compound **2**, which was found to be a SAM-competitive inhibitor of PRC2 methyltransferase activity (Figure 2). The commonality of the benzoyl amide motif between **1** and **2** led us to test the interchangeability of the tetramethylpiperidine (TMP) with the dimethylpyridone as in compound **3**. While significant potency was lost relative to **1**, amalgamated compound **3** had improved potency relative to **2**. While the chloro, cyano, and pyridazine substituents are important for potency in the TMP scaffold (**1**), removal of these substituents, to afford biphenyl ether **4**, enhanced potency in the dimethylpyridone series.

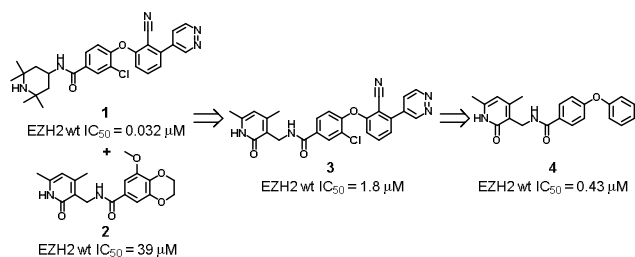


Figure 2. Merge of compound **1** with HTS hit **2**.

Given the potency disparity between **1** and **3**, it was clear that the structure activity relationships (SAR) from the tetramethylpiperidinyl benzamide series could not be applied to the emerging dimethylpyridone series. A brief screen of linkers between the two phenyl rings revealed that a carbon-bridged linker provided a 3-fold boost in potency (**5**, Table 1). In order to lower the logP and move the series into more drug-like chemical property space, polarity was introduced on the central ring.<sup>21</sup> This effort afforded pyridone **6** which retained similar activity to carbon-linked **5**. We then contracted the pyridone to a pyrazole (**7**) which led to a ~6-fold decrease in activity and using a 3-indolyl group (**8**) resulted in further loss of potency. However, inclusion of a 2-methyl group on indole **9** achieved a 126-fold improvement in potency to provide a compound with sub-100 nM activity against both wild-type (wt) and mutant EZH2. As methyl substitution at the 2-position of the indole afforded such a large potency increase, we investigated replacing the methyl group with other small substituents. A variety of functional groups spanning a range of physical properties were tested, but none of the replacements were tolerated.<sup>22</sup> Relaxed coordinate scan derived conformation energy profiles suggest that inclusion of the 2-methyl group impacts the rotational flexibility of the amide, significantly biasing the system towards one rotamer. In addition, the 2-methyl serves to tilt the amide bond out of the plane of the indole; these conformational effects appear essential to achieving potent inhibition of EZH2.<sup>23</sup>

Table 1. Genesis of the indole scaffold.

Compound	Structure	EZH2 wt IC <sub>50</sub> (μM) <sup>a</sup>	EZH2 Y641N IC <sub>50</sub> (μM) <sup>a</sup>
5		0.153 ± 0.013	0.795 <sup>b</sup>
6		0.094 <sup>b</sup>	1.35 <sup>b</sup>
7 <sup>c</sup>		0.604 ± 0.453	5.55 ± 1.34
8		1.64 <sup>b</sup>	>10 <sup>b</sup>
9		0.013 ± 0.008	0.062 ± 0.011

<sup>a</sup> IC<sub>50</sub> values reported as an average ≥2 determinations with standard deviation reported (SD). <sup>b</sup> Single measurement, no standard deviation reported. <sup>c</sup> Single unknown stereoisomer.

Subsequent SAR efforts focused on substitution of the indole nitrogen. Initially we separated the two enantiomers of **9** to afford **10** and **11** (Table 2). Both compounds were quite potent with IC<sub>50</sub> values less than 50 nM against wild-type EZH2. The *R* enantiomer (**10**) was modestly preferred and provided a compound with submicromolar cell potency in a HeLa H3K27me3 mechanism of action (MOA) assay. Further profiling of compound **10** in our *in vitro* ADME assays showed high microsomal metabolism, perhaps attributable to its lipophilicity (ClogP = 3.8<sup>24</sup>) of this compound. Further efforts were focused

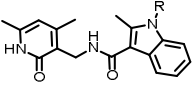
on increasing EZH2 potency with concomitant improvement in the physical properties of the series.<sup>25</sup>

Our efforts to modify the physical properties of these compounds focused on the indole side chain. Initially, the benzyl group of **10** was replaced with a variety of heterocycles, including pyrazole (**12**) and 2-pyridine (**13**). While this effort afforded compounds with improved microsomal stability relative to **10**, in general heteroaromatic substitutions were poorly tolerated and resulted in potency losses of approximately 5 fold in our biochemical assay. We next simplified the side chain to afford isopropyl derivative **14**, however this modification led to significant losses in biochemical potency. Potency could be regained by extending the chain of the isopropyl group by one

carbon to afford *sec*-butyl compound **15** which had micromolar cell activity and improved ADME compared to **10**.

Polar saturated systems were next investigated, including amide **16** and methoxy ether **17** (Table 2). Amide **16** had limited activity against EZH2 while compound **17** demonstrated similar biochemical and cellular potency to **10**. With methoxy ether **17** we had successfully lowered the ClogP to an acceptable range (ClogP = 2.2) while maintaining activity, but despite this improvement in physical properties compound **17** still displayed high microsomal metabolism. Further efforts to increase the stability of our EZH2 inhibitors focused on investigation of cyclic saturated systems.

Table 2: Indole side-chain SAR.



Compound	R	EZH2 wt ( $\mu\text{M}$ ) <sup>a</sup>	EZH2 Y641N ( $\mu\text{M}$ ) <sup>a</sup>	HeLa ( $\mu\text{M}$ ) <sup>b</sup>	Cl <sub>int</sub> (m/r/d/h) ( $\mu\text{L}/\text{min}/\text{mg}$ ) <sup>c</sup>	PPB (m/r/d/h) (% bound) <sup>c,d</sup>
9		0.013 $\pm$ 0.008	0.062 $\pm$ 0.011	n.t.	n.t.	n.t.
10		0.007 $\pm$ 0.004	0.034 $\pm$ 0.012	0.484 <sup>e</sup>	953/755/n.t./400	98/98/n.t./99
11		0.022 $\pm$ 0.002	0.097 $\pm$ 0.085	n.t.	n.t.	n.t.
12		0.073 $\pm$ 0.020	0.388 $\pm$ 0.051	n.t.	229/92/41/84	86/80/77/98
13		0.076 $\pm$ 0.032	0.358 $\pm$ 0.126	n.t.	349/47/n.t./72	88/88/n.t./98
14		0.159 <sup>e</sup>	0.512 <sup>e</sup>	n.t.	966/156/64/116	95/92/91/97
15		0.014 $\pm$ 0.013	0.118 $\pm$ 0.054	0.929 <sup>e</sup>	154/235/n.t./209	97/94/n.t./99
16		1.76 <sup>e</sup>	>10 <sup>e</sup>	n.t.	279/115/54/111	75/64/61/87
17		0.005 $\pm$ 0.003	0.043 $\pm$ 0.010	0.703 <sup>e</sup>	534/404/n.t./114	84/73/n.t./91

<sup>a</sup> IC<sub>50</sub> values reported as an average  $\geq 2$  determinations with standard deviation reported (SD). <sup>b</sup> The MOA cell assay measures global H<sub>3</sub>K27me<sub>3</sub> levels in HeLa cells; see supporting information. <sup>c</sup> m/r/d/h = mouse/rat/dog/human. <sup>d</sup> Plasma protein binding <sup>e</sup> Single measurement, no standard deviation reported. n.t. = not tested.

SAR studies on cyclic saturated systems<sup>26</sup> began with THP **18** which demonstrated excellent biochemical and cellular potency, but as with our other potent inhibitors, displayed high levels of microsomal metabolism *in vitro* (Table 3). Searching for a stable saturated system, a series of piperidine analogs were synthesized (**19** and **20**). The *N*-methyl piperidine derivative (**19**) was biochemically potent and had very low microsomal metabolism, but performed poorly in our cellular assay. In contrast to piperidine **19**, sulfonamide **20** showed excellent biochemical and cellular potency with an EC<sub>50</sub> of less than 100 nM. However **20** still had high microsomal metabolism in our ADME assays despite its reasonable ClogP (2.6). Since saturated heterocycles **18** and **20** afforded better physical properties but did not provide

improved microsomal stability, we turned our attention to modification of the pyridone.

Initially, we replaced the dimethylpyridone of **18** with a methoxypyridone to afford **21** (Table 3). Methoxypyridone **21** retained biochemical and cellular activity and provided a significant improvement in microsomal stability relative to the parent (**18**). The enhancement in microsomal stability imparted by the methoxypyridone translated to the piperidine series, as ethyl sulfonamide **22** also presented improved microsomal stability while retaining cellular activity. We investigated several other pyridone modifications, including an *n*Pr-pyridone (**23**) and a trifluoroethoxypyridone (**24**) but both the *n*Pr and

trifluoroethoxy pyridones led to diminished cellular potency relative to the methoxy pyridone-containing compounds.

Table 3: Pyridone-indole SAR.

Compound	R <sup>1</sup>	R <sup>2</sup>	EZH2 wt ( $\mu\text{M}$ ) <sup>a</sup>	EZH2 Y641N ( $\mu\text{M}$ ) <sup>a</sup>	H3K27me3 HeLa ( $\mu\text{M}$ ) <sup>b</sup>	Cl <sub>int</sub> (m/r/d/h) ( $\mu\text{L}/\text{min}/\text{mg}$ ) <sup>c</sup>	PPB (m/r/d/h) (% bound) <sup>c,d</sup>
18	Me		<0.001 <sup>e</sup>	0.004 <sup>e</sup>	0.098	729/277/182/251	95/86/77/94
19	Me		0.002 $\pm$ 0.0003	0.007 $\pm$ 0.003	0.568 $\pm$ 0.470	<7/<7/<7/<7	52/41/58/70
20	Me		0.001 $\pm$ 0.0002	0.003 $\pm$ 0.002	0.059 $\pm$ 0.020	428/303/77/254	95/91/76/95
21	OMe		0.002 $\pm$ 0.001	0.004 $\pm$ 0.002	0.075 $\pm$ 0.030	166/138/106/110	83/66/n.t./90
22	OMe		0.002 $\pm$ 0.0004	0.003 $\pm$ 0.002	0.080 $\pm$ 0.032	91/35/31/59	94/84/75/92
23	nPr		0.005 $\pm$ 0.004	0.040 $\pm$ 0.005	0.266 $\pm$ 0.009	1665/928/283/794	99/97/95/98
24	OCH <sub>2</sub> CF <sub>3</sub>		0.040 <sup>e</sup>	0.485 <sup>e</sup>	1.08 <sup>e</sup>	n.t.	n.t.
EPZ-6438 <sup>16</sup>	-	-	0.001 $\pm$ 0.0004	0.001 $\pm$ 0.0002	0.020 $\pm$ 0.010	-	-
GSK-126 <sup>13</sup>	-	-	0.001 $\pm$ 0.0004	0.002 $\pm$ 0.001	0.280 $\pm$ 0.080	-	-

<sup>a</sup> IC<sub>50</sub> values reported as an average  $\geq 2$  determinations with standard deviation reported (SD). <sup>b</sup> Our MOA cell assay measures global H3K27me3 levels in HeLa cells; see supporting information. <sup>c</sup> m/r/d/h = mouse/rat/dog/human. <sup>d</sup> Plasma protein binding <sup>e</sup> Single measurement, no standard deviation reported. n.t = not tested.

Ethyl sulfonamide **22** was chosen for profiling in mice due to its excellent cellular potency and reasonable ADME properties. Mouse IV PK of **22** showed a clearance of 2.74 L/h/kg, a reasonable volume (0.795 L/kg), and short half-life of 0.37 h (Figure 3A). Given the clearance of **22** in mice we suspected that even high doses of **22** given via oral administration (PO) would not afford the exposure necessary to see target engagement *in vivo*. As a means of achieving higher exposures and a longer half-life we dosed compound **22** subcutaneously (SC). We were pleased to see that when given to mice at 200 mpk SC compound **22** showed a prolonged half-life and excellent AUC with a free-fraction above the cellular EC<sub>50</sub> out to 16 hours.

With this result in hand we advanced sulfonamide **22** into our KARPAS-422 pharmacodynamic (PD) model.<sup>27</sup> The KARPAS-

422 PD experiment with **22** was run for 17 days with 200 mg/kg BID dosing. After 17 days the tumors were harvested and the level of H3K27me3 was analyzed at 1 hour post last dose and compound concentrations were analyzed at 1, 6, and 12 hours post last dose. Compound **22** showed ~84% reduction in H3K27me3 mark relative to vehicle control, demonstrating a profound and prolonged inhibition of EZH2 *in vivo* (Figure 3B). This strong PD effect, as measured by the decrease in H3K27me3 levels, was achieved by maintaining the plasma and tumor concentrations of **22** over the cellular EC<sub>50</sub> (Figure 3C). Based on these encouraging results we subsequently advanced compound **22** into our KARPAS-422 efficacy model.

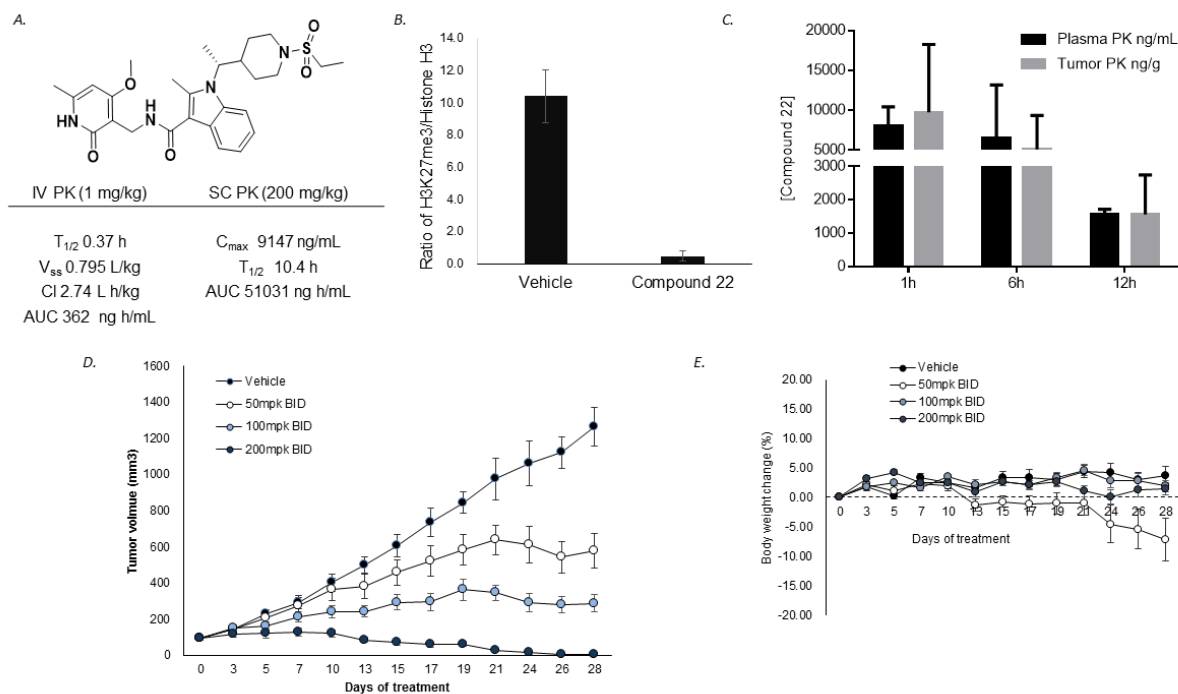


Figure 3: PK data, KARPAS-422 PD, and KARPAS-422 efficacy data of compound **22**; A. Mouse PK data of **22**; B. Ratio of H3K27me3 to histone H3 in the KARPAS-422 PD study for vehicle and treated arms.; C. Time course of tumor and plasma concentrations of compound **22** from the KARPAS-422 PD study at 1, 6, and 12 h post last dose.; D. Dose-response from the KARPAS-422 efficacy study.; E. Body-weight curves of the individual arms from the efficacy study

The *in vivo* efficacy of sulfonamide **22** was examined in a KARPAS-422 mouse xenograft model (Figure 3). Compound **22** was dosed at 50 mg/kg, 100 mg/kg, and 200 mg/kg via SC administration following a twice daily dosing schedule (BID). Dosing of sulfonamide **22** for 28 days resulted in a dose-dependent reduction in tumor volume with tumor growth inhibitions (TGI) of 54%, 77%, and >100% (regression), respectively when compared to the vehicle arm (Figure 3D).<sup>28</sup> Treatment with **22** was tolerated at all doses studied with less than 10% body-weight loss observed during the course of treatment (Figure 3E). The high efficacy and low toxicity of compound **22** make it a useful tool compound for studying the effect of EZH2 inhibition in both *in vitro* and *in vivo* contexts.

In summary, starting from HTS hit **2** (EZH2 IC<sub>50</sub> = 39  $\mu$ M) this report describes the identification of a series of indole-based EZH2 inhibitors. Optimization of this series afforded sulfonamide **22**, a highly potent inhibitor of EZH2. Compound **22** shows good activity in our KARPAS-422 PD and efficacy models at well-tolerated doses, making it a useful tool compound to explore the *in vivo* effects of EZH2 inhibition. Further efforts describing the optimization of this indole series will be reported in due course.

## References and notes

- Jones, P. A.; Baylín, S. B. *Cell* 2007, 128, 683.
- Margueron, R.; Reinberg, D. *Nature* 2011, 469, 343.
- Kleer, C. G.; Cao, Q.; Varambally, S.; Shen, R.; Ota, I.; Tomlins, S. A.; Ghosh, D.; Sewalt, R. G.; Otte, A. P.; Hayes, D. F.; Sabel, M. S.; Livant, D.; Weiss, S. J.; Rubin, M. A.; Chinnaiyan, A. M. *Proc. Natl. Acad. Sci. U.S.A.* 2003, 100, 11606.
- Varambally, S.; Dhanasekaran, S. M.; Zhou, M.; Barrette, T. R.; Kumar-Sinha, C.; Sanda, M. G.; Ghosh, D.; Pienta, K. J.; Sewalt, R. G.; Otte, A. P.; Rubin, M. A.; Chinnaiyan, A. M. *Nature* 2002, 419, 624.
- Majer, C. R.; Jin, L.; Scott, M. P.; Knutson, S. K.; Kuntz, K. W.; Keilhack, H.; Smith, J. J.; Moyer, M. P.; Richon, V. M.; Copeland, R. A.; Wigle, T. J. *FEBS Lett.* 2012, 586, 3448.
- McCabe, M. T.; Graves, A. P.; Ganji, G.; Diaz, E.; Halsey, W. S.; Jiang, Y.; Smitheman, K. N.; Ott, H. M.; Pappalardi, M. B.; Allen, K. E.; Stephanie, B. C.; Della Pietra, A., III; Dul, E.; Hughes, A. M.; Gilbert, S. A.; Thrall, S. A.; Tummino, P. J. *Proc. Natl. Acad. Sci. U.S.A.* 2012, 109, 2989.
- Sneeringer, C. J.; Scott, M. P.; Kuntz, K. W.; Knutson, S. K.; Pollock, R. M.; Richon, V. M.; Copeland, R. A. *Proc. Natl. Acad. Sci. U.S.A.* 2010, 107, 20980.
- Wigle, T. J.; Knutson, S. K.; Jin, L.; Kuntz, K. W.; Pollock, R. M.; Richon, V. M.; Copeland, R. A.; Scott, M. P. *FEBS Lett.* 2011, 585, 3011.
- Yap, D. B.; Chu, J.; Berg, T.; Schapira, M.; Cheng, S. W.; Moradian, A.; Morin, R. D.; Mungall, A. J.; Meissner, B.; Boyle, M.; Marquez, V. E.; Marra, M. A.; Gascoyne, R. D.; Humphries, R. K.; Arrowsmith, C. H.; Morin, G. B.; Aparicio, S. A. *J. R. Blood* 2011, 117, 2451.
- McCabe, Michael T.; Creasy, Caretha L. *Epigenomics* 2014, 6, 341.
- Diaz, E.; Machutta, C. A.; Chen, S.; Jiang, Y.; Nixon, C.; Hofmann, G.; Key, D.; Sweitzer, S.; Patel, M.; Wu, Z.; Creasy, C. L.; Kruger, R. G.; LaFrance, L.; Verma, S. K.; Pappalardi, M. B.; Le, B.; Van Aller, G. S.; McCabe, M. T.; Tummino, P. J.; Pope, A. J.; Thrall, S. H.; Schwartz, B.; Brandt, M. J. *Biomol. Screening* 2012, 17, 1279.
- Knutson, S. K.; Wigle, T. J.; Warholc, N. M.; Sneeringer, C. J.; Allain, C. J.; Klaus, C. R.; Sacks, J. D.; Raimondi, A.; Majer, C. R.; Song, J.; Scott, M. P.; Jin, L.; Smith, J. J.; Olhava, E. J.; Chesworth, R.; Moyer, M. P.; Richon, V. M.; Copeland, R. A.; Keilhack, H.; Pollock, R. M.; Kuntz, K. W. *Nat. Chem. Biol.* 2012, 8, 890.
- McCabe, M. T.; Ott, H. M.; Ganji, G.; Korenchuk, S.; Thompson, C.; Van Aller, G. S.; Liu, Y.; Graves, A. P.; Della Pietra, A., III; Diaz, E.; LaFrance, L. V.; Mellinger, M.; Duquenne, C.; Tian, X.; Kruger, R. G.; McHugh, C. F.; Brandt, M.; Miller, W. H.; Dhanak, D.; Verma, S. K.; Tummino, P. J.; Creasy, C. L. *Nature* 2012, 492, 108.
- Qi, W.; Chan, H.; Teng, L.; Li, L.; Chuai, S.; Zhang, R.; Zeng, J.; Li, M.; Fan, H.; Lin, Y.; Gu, J.; Ardayfio, O.; Zhang, J.-H.; Yan, X.; Fang, J.; Mi, Y.; Zhang, M.; Zhou, T.; Feng, G.; Chen, Z.; Li, G.; Yang, T.; Zhao, K.; Liu, X.; Yu, Z.; Lu, C.; Atadja, P.; Li, E. *Proc. Natl. Acad. Sci. U.S.A.* 2012, 109, 21360.

15. Verma, S. K.; Tian, X.; LaFrance, L. V.; Duquenne, C.; Suarez, D. P.; Newlander, K. A.; Romeril, S. P.; Burgess, J. L.; Grant, S. W.; Brackley, J. A.; Graves, A. P.; Scherzer, D. A.; Shu, A.; Thompson, C.; Ott, H. M.; Van Aller, G. S.; Machutta, C. A.; Diaz, E.; Jiang, Y.; Johnson, N. W.; Knight, S. D.; Kruger, R. G.; McCabe, M. T.; Dhanak, D.; Tummino, P. J.; Creasy, C. L.; Miller, W. H. *ACS Med. Chem. Lett.* 2012, 3, 1091.
16. Konze, K. D.; Ma, A.; Li, F.; Barsyte-Lovejoy, D.; Parton, T.; MacNevin, C. J.; Liu, F.; Gao, C.; Huang, X.-P.; Kuznetsova, E.; Rougie, M.; Jiang, A.; Pattenden, S. G.; Norris, J. L.; James, L. I.; Roth, B. L.; Brown, P. J.; Frye, S. V.; Arrowsmith, C. H.; Hahn, K. M.; Wang, G. G.; Vedadi, M.; Jin, J. *ACS Chem. Biol.* 2013, 8, 1324.
17. Knutson, S. K.; Kawano, S.; Minoshima, Y.; Warholc, N. M.; Huang, K.-C.; Xiao, Y.; Kadowaki, T.; Uesugi, M.; Kuznetsov, G.; Kumar, N.; Wigle, T. J.; Klaus, C. R.; Allain, C. J.; Raimondi, A.; Waters, N. J.; Smith, J. J.; Porter-Scott, M.; Chesworth, R.; Moyer, M. P.; Copeland, R. A.; Richon, V. M.; Uenaka, T.; Pollock, R. M.; Kuntz, K. W.; Yokoi, A.; Keilhack, H. *Mol. Cancer Ther.* 2014, 13, 842.
18. Sweis, R. F.; Michaelides, M. R. *Annu. Rep. Med. Chem.* 2013, 48, 185.
19. Campbell, J. E.; Kuntz, K. W.; Knutsen, S. K.; Warholc, N. M.; Keilhack, H.; Wigle, T. J.; Raimondi, A.; Klaus, C. R.; Rioux, N.; Yokoi, A.; Kawano, S.; Minoshima, Y.; Choi, H.-W.; Scott, M. P.; Waters, N. J.; Smith, J. J.; Chesworth, R.; Moyer, M. P.; Copeland, R. A. *ACS Med. Chem. Lett.* 2015, 6, 491.
20. Nasveschuk, C. G.; Gagnon, A. G.; Garapaty-Rao, S.; Balasubramanian, S.; Campbell, R.; Lee, C.; Zhao, F.; Bergeron, L.; Cummings, R.; Trojer, P.; Audia, J. E.; Albrecht, B. K.; Harmange, J.-C. P. *ACS Med. Chem. Lett.* 2014, 5, 378.
21. Wenlock, M. C.; Austin, R. P.; Barton, P.; Davis, A. M.; Leeson, P. D. A. *J. Med. Chem.* 2003, 46, 1250.
22. For a review on methyl effects in drug discovery, see: Schönherr, Heike; Cernak, Tim *Angew. Chem. Int. Ed.* 2013, 52, 2.
23. Gas phase conformational energies calculated using Jaguar version 8.2, release 12, Schrödinger, Inc., New York, NY (DFT(b3lyp) method with cc-pvtz(-f)++ basis set). Further details can be found in the supporting information.
24. Calculated using Chemdraw 13.0.
25. Meanwell, N. A. *Chem. Res. Toxicol.* 2011, 24, 1420.
26. For synthetic procedures see the supporting information.
27. Further information on the KARPAS PD and efficacy models can be found in the supporting information.
28. The body weight loss observed in the 50 mpk arm is the result of three animals. These animals bore tumors showing ulceration which may have resulted in loss of body fluid and compromised their ability to move and feed leading to non-drug related weight loss.